

Molecular modulation in a hollow fiber

S. Sensarn, S. N. Goda, G. Y. Yin, and S. E. Harris

Edward L. Ginzton Laboratory, Stanford University, Stanford, California 94305

Received June 26, 2006; revised July 18, 2006; accepted July 20, 2006;
posted July 20, 2006 (Doc. ID 72338); published September 11, 2006

We report the extension of the technique of molecular modulation to a deuterium-filled optical fiber. Using driving lasers at 807 and 1064 nm, each with a pulse energy of several millijoules and a 200 μm diameter fiber with a length of 22.5 cm, we generate 12 sidebands with wavelengths spanning 1.56 μm to 254 nm.

© 2006 Optical Society of America

OCIS codes: 060.4370, 190.5650, 230.6080.

The technique of molecular modulation employs two driving lasers whose frequency difference is close, but not equal, to that of a Raman transition. Because they are detuned from the resonance, these lasers adiabatically drive the molecular transition and thereby modulate the electronic polarizability. To first order, the incident laser beams are phase modulated and generate a comb of sidebands that have Bessel function spectral amplitudes.^{1,2} By using variations of the original technique termed as multiplicative and additive, hundreds of sidebands with a spectral range of four octaves may be generated.^{3,4} It has been shown that the phases of these sidebands may be modified to produce synthesized waveforms and optical pulses as short as a single cycle.^{5,6}

To obtain the necessary coherence on the molecular transition, driving lasers must have power densities of several GW/cm^2 . For a free-space interaction length of 25 cm and a Q -switched pulse length of 15 ns, the necessary driving laser pulse energy is about 100 mJ.

This Letter reports the demonstration of molecular modulation using a hollow deuterium-filled optical fiber. We drive the fundamental vibrational transition of deuterium using laser pulse energies of several millijoules incident on a 22.5 cm long, 200 μm diameter fused silica fiber. We generate 12 sidebands with wavelengths from 1.56 μm to 254 nm. Compared with generation in free space with the same beam waist, this fiber extends the interaction length by a factor of six, thereby allowing generation with millijoules of incident pulse energy.

There is now extensive literature demonstrating the use of hollow optical fibers for the enhancement of nonlinear optical processes. Following the demonstration by Miles *et al.* in 1974,⁷ these fibers now play an important role in areas such as high-energy laser pulse compression^{8,9} and high-order harmonic generation.^{10,11} The use of hollow fibers in the generation of ultrashort pulses has been studied in great detail.¹² As it bears on this work, Burzo *et al.* described the use of a hollow fiber to enhance molecular modulation in deuterium.¹³ Raman generation in hollow fibers by use of submillijoule, ultrashort pulses to drive Raman transitions in the transient regime has been reported.^{14–16}

Our experimental setup is shown in Fig. 1. The hollow optical fiber (Polymicro Technologies

TSPE200350) rests on a brass V-groove mount inside a 2.54 cm outer diameter, 58.7 cm long thin-wall stainless-steel tube. The V-groove keeps the fiber straight, which prevents optical loss and excitation into high-order modes. Steel shims placed on top of the groove prevent the fiber from bending vertically but allow it to slide as the brass contracts from cooling. An insulated steel cooling chamber surrounds the center portion of the tube where the fiber is located. The chamber is filled with liquid nitrogen for cooling. The tube is filled with 200 Torr deuterium gas, which surrounds and fills the hollow fiber. Since the brass mount is in contact with both the tube and the fiber, it serves as a thermal pathway to cool the fiber and the deuterium gas inside.

We use two solid-state lasers that are nearly two-photon resonant with the fundamental vibrational transition in deuterium. The 1064 nm laser is an injection-seeded, Q -switched Quanta-Ray GCR-290 Nd:YAG laser with a 12 ns pulse width and a calculated linewidth of 37 MHz. The 807 nm laser is a custom injection-seeded Ti:sapphire laser with a 16 ns, nearly Gaussian pulse width. The lasers are combined on a beam splitter and aligned through a 25 cm lens into the fiber. The alignment path is set by a backward-coupled He–Ne laser that excites the fundamental EH_{11} mode of the hollow fiber. The focused spot sizes are 150 μm for the 1064 nm laser and 120 μm for the 807 nm laser. Each laser is attenuated to provide incident pulse energies of 2.8 mJ at the input of the fiber. The two-photon detuning from the vibrational Raman transition at 2994 cm^{-1} is varied by adjusting the frequency of the 807 nm laser. With the detuning set at 230 MHz below resonance, we generate 12 sidebands from 1.56 μm to 254 nm. A

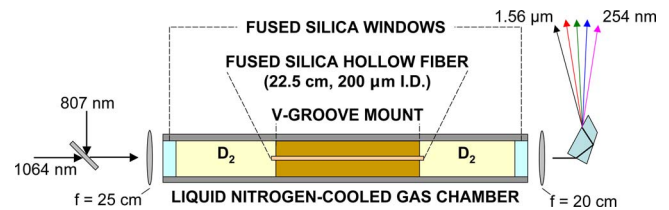


Fig. 1. (Color online) Experimental setup. Drive lasers are combined on a dichroic beam splitter. UV-grade fused silica lenses focus the drive lasers into the laser-cleaved hollow fiber and focus the output light onto a pyroelectric detector (not shown). The gas chamber is filled with 200 Torr deuterium.

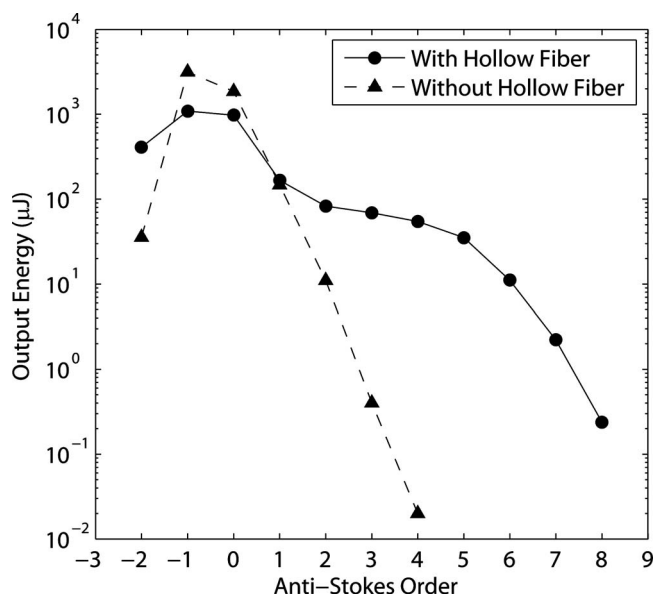


Fig. 2. Energy of generated sidebands at the output of the gas cell with and without a hollow fiber. The input drive energies are 2.8 mJ for each drive laser. The 1064 and 807 nm drive wavelengths are labeled as -1 and 0, respectively.

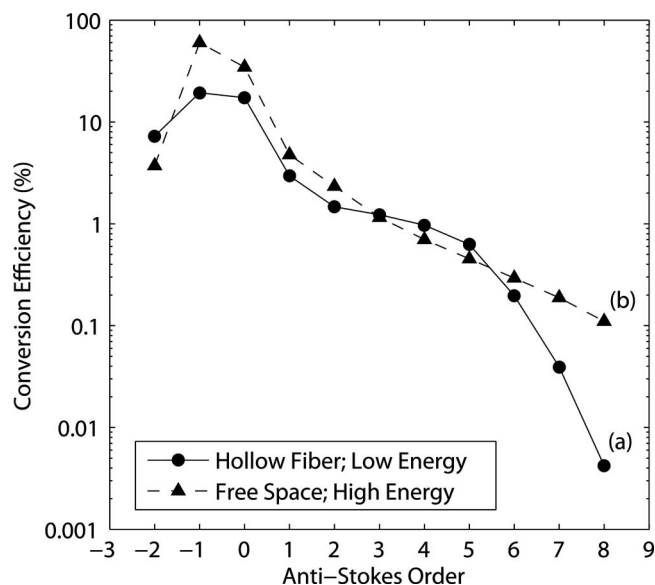


Fig. 3. Percentage of total incident energy converted to sideband energy. Generation is shown (a) in a hollow fiber with 5.8 mJ total incident energy and (b) in free space with 120 mJ total incident energy and a 30 cm confocal parameter.



Fig. 4. Spatial modes of generated sidebands projected onto a white screen. Sideband wavelengths from left to right are 807 (faint), 650, 544, 488, 410, 365, 330, and 300 nm. The 650, 544, 488, and 410 nm beams have been attenuated by a factor of 10 with a neutral-density filter.

20 cm lens is used at the output of the chamber to re-focus the diffracting sidebands through a Pellin-Broca prism and onto a pyroelectric detector.

Figure 2 shows the generated energies in each sideband with the fiber present and with it removed. The two-photon detuning is optimized to produce the widest bandwidth in both cases. The optimal detunings are 230 MHz below resonance in the hollow fiber and 100 MHz below resonance in free space. With the hollow fiber in place, 11 sidebands have energies above $0.1 \mu\text{J}$. The remaining 254 nm sideband is visible when focused onto a fluorescing card. Figure 2 shows a strong increase in generation efficiency from the hollow-fiber guiding. Generation into the fourth anti-Stokes sideband is $48 \mu\text{J}$ in the hollow fiber compared with 20 nJ in free space.

Note that the total energy in all sidebands drops by almost half when the fiber is present. The lower total output energy is primarily due to coupling and propagation losses associated with the hollow fiber. Measuring the fiber input and output energies for the two drive lasers independently yields a total energy transmittance of 62%. When the drive lasers propagate together, the total output energy including all sidebands is 51% of the incident energy. We believe that coupling of generated sidebands into higher-order spatial modes and significant propagation loss

at $1.56 \mu\text{m}$ (21% for an ideal hollow fiber with our dimensions) are responsible for the additional loss.

We have also performed experiments with five different gas pressures ranging from 157 to 375 Torr, and we find that 200 Torr is the optimal pressure. We use the generated energy in the fourth anti-Stokes sideband as a metric for optimizing gas pressure.

Figure 3 compares generation efficiency in a hollow fiber with an optimized experiment in free space where large interaction lengths and intensities are achieved with loose focusing and high energy. Similarly to previous free-space experiments,⁴ we loosely focus the same two drive lasers into a 75 cm long chamber filled with 50 Torr deuterium gas. The drive energies are 65 mJ for the 1064 nm laser and 56 mJ for the 807 nm laser. The focused spot sizes are $460 \mu\text{m}$ for the 1064 nm laser and $400 \mu\text{m}$ for the 807 nm laser with confocal parameters of about 30 cm. To directly compare the low-energy hollow fiber and high-energy free-space experiments, we define conversion efficiency for a particular sideband as the percentage of total incident energy converted into that sideband. By this definition, fiber losses due to coupling and propagation reduce generation efficiency. Despite fiber-related losses, and at 20 times lower incident energy, the generation efficiency in the hollow fiber is roughly equal to that in free space.

Figure 4 shows a photograph of sidebands generated by a laser-cleaved hollow fiber. The beams are nearly collimated by a 25 cm fused silica lens placed 20 cm from the fiber output and are separated by a fused silica prism. This figure is representative of the best spatial mode quality we have achieved. Spatial mode quality varies unpredictably with different fibers, although laser-cleaved fibers generally perform better than hand-cleaved fibers. We note that higher-order sidebands have somewhat degraded spatial modes.

Raman generation in a hollow fiber is robust. A laser-cut fiber without end-face defects is operative for many hours at 5.6 mJ of incident energy. There is little degradation of spatial mode or generation efficiency. When examined with a 20 \times microscope objective, there is very slight burn damage to the polyimide coating on the input end of the fiber. Hand-cleaved fibers show more significant damage. We find that the quality of the spatial mode of the backward-coupled He–Ne laser is a good indicator of hollow-fiber performance. Fibers that cannot support a clean EH₁₁ He–Ne mode show more damage than those that do.

The generation efficiency in a hollow optical fiber will improve at higher input energies and longer fiber lengths. At present we find that the end-face burning of the fiber limits our input energy to about 6 mJ. We anticipate experiments aimed at improving the coupling efficiency and increasing the fiber length. Significant increases in length may be possible. It is likely that hollow fibers may allow an increase in the repetition rate of broadband light sources that are based on molecular modulation from the present-day 10 Hz to the kilohertz range. For applications at higher power, tapered fibers may allow the input energy to be raised significantly.

We thank Orazio Svelto for his encouragement and suggestions and Alexei Sokolov for a preprint of Ref.

13. The experiments described in this Letter were completed before receiving this preprint. This work was supported by the U.S. Army Research Office and the U.S. Air Force Office of Scientific Research. S. Sensarn's e-mail address is sensarn@stanford.edu.

References

1. S. E. Harris and A. V. Sokolov, *Phys. Rev. Lett.* **81**, 2894 (1998).
2. A. V. Sokolov, D. R. Walker, D. D. Yavuz, G. Y. Yin, and S. E. Harris, *Phys. Rev. Lett.* **85**, 562 (2000).
3. D. D. Yavuz, D. R. Walker, M. Y. Shverdin, G. Y. Yin, and S. E. Harris, *Phys. Rev. Lett.* **91**, 233601 (2003).
4. A. V. Sokolov, M. Y. Shverdin, D. R. Walker, D. D. Yavuz, A. M. Burzo, G. Y. Yin, and S. E. Harris, *J. Mod. Opt.* **52**, 285 (2005).
5. A. V. Sokolov, D. R. Walker, D. D. Yavuz, G. Y. Yin, and S. E. Harris, *Phys. Rev. Lett.* **87**, 033402 (2001).
6. M. Y. Shverdin, D. R. Walker, D. D. Yavuz, G. Y. Yin, and S. E. Harris, *Phys. Rev. Lett.* **94**, 033904 (2005).
7. R. B. Miles, G. Laufer, and G. C. Bjorklund, *Appl. Phys. Lett.* **30**, 417 (1977).
8. M. Nisoli, S. D. Silvestri, and O. Svelto, *Appl. Phys. Lett.* **68**, 2793 (1996).
9. B. Schenkel, J. Biegert, U. Keller, C. Vozzi, M. Nisoli, G. Sansone, S. Stagira, S. D. Silvestri, and O. Svelto, *Opt. Lett.* **28**, 1987 (2003).
10. T. Pfeifer, R. Kemmer, R. Spitzenpfeil, D. Walter, C. Winterfeldt, G. Gerber, and C. Spielmann, *Opt. Lett.* **30**, 1497 (2005).
11. Y. Tamaki, Y. Nagata, M. Obara, and K. Midorikawa, *Phys. Rev. A* **59**, 4041 (1999).
12. A. M. Zheltikov, *Phys. Usp.* **45**, 687 (2002).
13. A. M. Burzo, A. V. Chugreev, and A. V. Sokolov, *Opt. Commun.* **264**, 454 (2006).
14. A. Nazarkin, G. Korn, M. Wittmann, and T. Elsaesser, *Phys. Rev. Lett.* **83**, 2560 (1999).
15. E. Sali, K. J. Mendham, J. W. G. Tisch, T. Halfmann, and J. P. Marangos, *Opt. Lett.* **29**, 495 (2004).
16. R. A. Bartels, T. C. Weinacht, N. Wagner, M. Baertschy, C. H. Greene, M. M. Murnane, and H. C. Kapteyn, *Phys. Rev. Lett.* **88**, 013903 (2002).